

A local metallic state in globally insulating $La_{1.24}Sr_{1.76}Mn_2O_7$ well above the metal-insulator transition

Z. Sun,^{1,2,*} J. F. Douglas,¹ A. V. Fedorov,² Y. -D. Chuang,² H. Zheng,³ J. F. Mitchell,³ and D. S. Dessau^{1,†}

¹Department of Physics, University of Colorado, Boulder, CO 80309, USA

²Advanced Light Source, Lawrence Berkeley National Laboratory, Berkeley, CA 94720, USA

³Materials Science Division, Argonne National Laboratory, Argonne, IL 60439, USA

(Dated: November 30, 2019)

In the spectacularly successful theory of solids, the distinction between metals, semiconductors, and insulators is based upon the behavior of the electrons nearest the Fermi level E_F , which separates the occupied from unoccupied electron energy levels. A metal has E_F in the middle of a band of electronic states, while E_F in insulators and semiconductors lies in the gap between states. The temperature-induced transition from a metallic to an insulating state is therefore generally connected to a vanishing of the low energy electronic states at E_F ¹. Using angle-resolved photoemission measurements from the “colossal magnetoresistive” (CMR) oxide $La_{1.24}Sr_{1.76}Mn_2O_7$, we here show the first direct evidence of a counter example, in which a significant density of states at E_F exists in the insulating regime above the critical temperature T_C . Further, small amounts of metallic spectral weight survive up to the temperature scale T^* more than twice the T_C of the system. Such behavior indicates the presence of local regions of metal phase separated out from an insulating background. This helps clarify many of the exotic properties of this materials, and may have close ties to a variety of exotic phenomena in other correlated electron systems including in particular the pseudogap scale T^* in underdoped cuprates².

As shown in figure 1a, the colossal magnetoresistive (CMR) oxide $La_{2-2x}Sr_{1+2x}Mn_2O_7$ ($x=0.38$) exhibits a metal insulator transition at a T_C of about 130K, at which point the system also switches from being a ferromagnet (low T) to a paramagnet (high T)³. We performed angle-resolved photoemission spectroscopy (ARPES) experiments on cleaved single crystals of these materials, with an experimental arrangement as described elsewhere⁴. ARPES is an ideal experimental probe of the electronic structure since it gives the momentum-resolved single-particle excitation spectrum. As discussed in ref. 4 the $x=0.38$ compound studied here does not contain the low energy pseudogap of the $x=0.4$ samples^{5,6,7,8}. The much larger metallic spectral weight of these non-pseudogapped compounds also allows us to study the electronic behavior in greater detail.

Figure 1c shows a large-energy-scale experimental picture of a low temperature $d_{x^2-y^2}$ symmetry band taken along the black cut near the zone boundary, as shown in the figure 1b. We are able to get clean data by isolat-

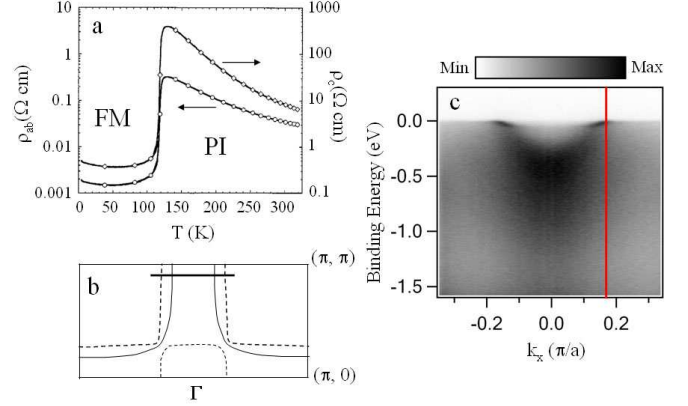


FIG. 1: Overview of features of $La_{1.24}Sr_{1.76}Mn_2O_7$. (a) Resistivity vs. temperature, after ref 3. (b) A representative Fermi surface. (c) Low temperature (20K) ARPES data over a large-energy-scale taken along the black cut near the zone boundary, as shown in (b).

ing the various bilayer-split bands using different photon energies, as described in ref. 4. In particular, in this paper we only show data from the antibonding bilayer-split band which has Fermi crossings at $k_x=\pm 0.17 \pi/a$, $k_y=0.9 \pi/a$, corresponding to the solid Fermi surface in figure 1b. The energy distribution curves (EDCs) at k_F (indicated by the red line in figure 1c) taken at a series of temperatures are shown in figure 2a. Figure 2b shows the identical spectra and identical scaling, but offset vertically for clarity. All spectra have been normalized only to the incident photon flux.

At low temperature, the EDCs clearly show a structure of peak-dip-hump, where the peak and the hump would nominally be considered the coherent part (quasiparticle) and “incoherent” part of the single particle spectrum respectively, as has been discussed for the spectra of the high T_C cuprate superconductors^{9,10,11}. One sees that the near- E_F spectral weight diminishes with increasing temperature, while the high binding energy (>700 meV) part is less affected by temperature. Contrary to the general picture of the metal-insulator transition, in which a gap develops in the single particle spectrum when an electronic system becomes insulating¹, the EDCs here still exhibit a sharp Fermi cutoff indicating metallic behavior at temperatures in which the macroscopic DC conductivity is characteristic of insulation (e.g. the spectra

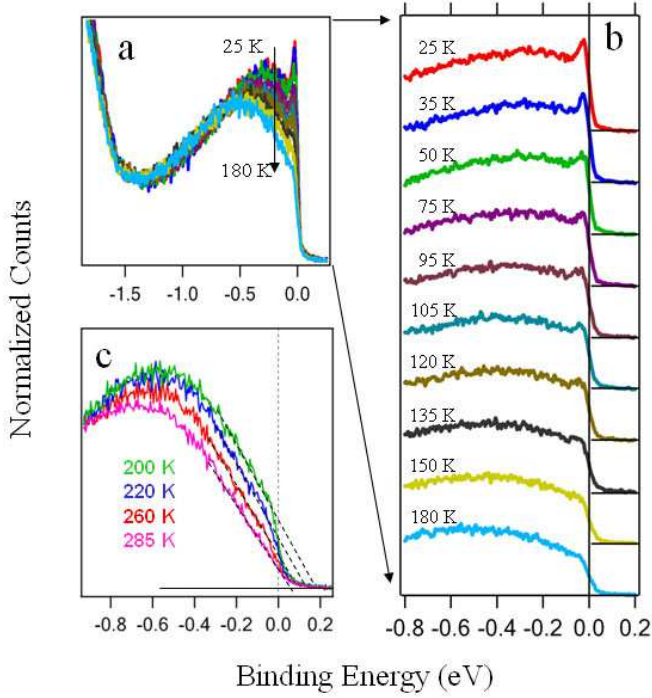


FIG. 2: Energy Distribution Curves (EDCs) as a function of temperature at k_F (red line of figure 1c), indicating metallic spectral weight above T_C . (a, b) the same data set scaled by the incident flux and are taken while warming. (c) EDCs from a different sample taken at the high temperature range. Clear breaks are seen in the spectral intensity near E_F for all but the highest temperature, indicating finite metallic spectral weight and a T^* just above 285K (see figure 3 for details of the T^* determination).

at 135, 150 and 180K). To our knowledge, this unusual behavior, a metallic Fermi edge in a globally insulating system, has not been previously observed on the insulating side of a metal-insulator transition. The opposite, in which a metallic system shows a lack of a Fermi cutoff, is on the other hand expected in exotic low-dimensional systems such as the Luttinger Liquids¹², and has likely been observed¹³. The other situation most likely to show a metallic Fermi edge in a globally insulating system is that of an Anderson-localized system beyond the mobility edge. However, in such systems a Coulomb gap is expected to remove the metallic weight near the Fermi energy¹⁴.

It should be pointed out that there is a remarkable difference between $La_{1.24}Sr_{1.76}Mn_2O_7$ and $La_{1.2}Sr_{1.8}Mn_2O_7$ samples. Quasiparticles have been found near the zone boundary at the doping levels of $x=0.36$ and 0.38 in $La_{2-2x}Sr_{1+2x}Mn_2O_7$, while there exists a large energy pseudogap in $x=0.4$ samples⁴. Temperature dependent studies have also been performed on $La_{1.2}Sr_{1.8}Mn_2O_7$ samples and have not shown evidence for metallic spectral weight above T_C ^{6,7,8}. Similar to high- T_C cuprates, physical properties exhibit strong vari-

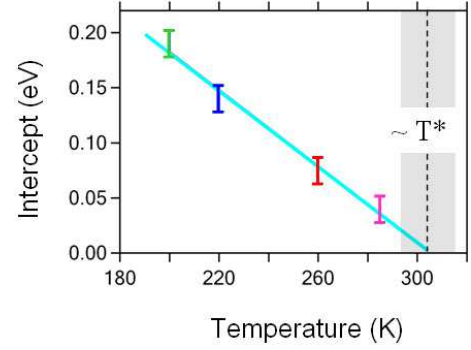


FIG. 3: Determination of T^* . Zero intensity intercepts as a function of temperature from the linear fits to the data shown in figure 2c. These intercepts go to zero at 305K, which we label as $T^* \sim 305K$.

ations with doping in manganites. The cause of the difference between $La_{1.24}Sr_{1.76}Mn_2O_7$ and $La_{1.2}Sr_{1.8}Mn_2O_7$ samples is still not understood yet.

On a different sample we have done higher temperature scans, looking for a possible temperature scale at which the metallic spectral weight disappears. This data is shown in figure 2c and shows a clear discontinuity in the slope near the Fermi energy for all but the 285K data, indicating a finite metallic spectral weight. This effect is emphasized by an extrapolation of the spectral weight using a simple linear fit to the data between -0.3 and -0.05 eV, as shown by the dotted lines in the figure. Upon raising the sample temperature we see that the intercept of these dotted lines with the horizontal axis decreases at an approximately linear rate (figure 3). As shown in this figure these zero intensity intercepts reach the Fermi energy at $305 \pm 10K$. We thus indicate 305K as the temperature at which the first bits of metallic weight become apparent, which we indicate as the temperature T^* . Technical reasons including sample aging and excessive manipulator drift preclude us from making the full range of measurements on a single cleave. We therefore used different samples to study the electronic excitations in different temperature regimes.

One should consider whether it might be possible for the metallic spectral weight far above T_C to have originated from small bits of intergrowth of a higher T_C sample. This could not be from a layered manganite, as the max T_C of all known layered manganites is $\sim 160K$. A perovskite intergrowth with a $T_C \sim 300K$ could exist, though it is easy to discount the possibility of the high temperature dispersive ARPES signal originating from a perovskite intergrowth. Our high temperature data displays the same type of bilayer band splitting as our low temperature data (this Letter only presents the data from the antibonding component), which is a direct consequence of having two MnO_2 planes per unit cell. The perovskite samples have one MnO_2 plane per cell and so would not show the bilayer splitting. Additionally, it is

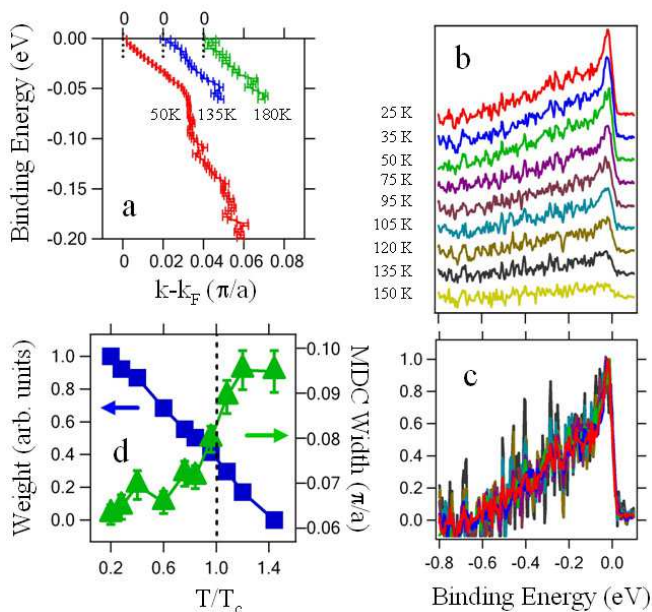


FIG. 4: Properties of the metallic portion of the sample. (a) Electronic dispersion showing a similar k_F , v_F and electron-phonon coupling as a function of temperature. (b, c) Metallic EDCs or M-EDCs obtained by subtracting the 180K EDC from all lower temperature data. (b) shows the raw scaling while (c) scales each spectrum to have a similar max intensity. (d) MDC widths (green triangles) and integrated M-EDC spectral weights (blue squares) as a function of temperature.

well known that the perovskite material does not cleave because it lacks the rock salt layer of the cleavable layered manganites. Indeed, to date ARPES has failed to show a dispersive band from a perovskite manganite.

Figure 4a shows the electronic dispersion of the near-Fermi states as a function of temperature obtained from an analysis of momentum distribution curves (MDCs). This data indicates that the main properties of the metal, such as the Fermi wave vector k_F , the Fermi velocity v_F , the electron phonon coupling parameter λ , and the effective mass m^* don't change significantly as a function of temperature, even as the metal-insulator transition temperature T_C is traversed. This is an unexpected behaviour for a metal-insulator transition in which these parameters would vary dramatically with temperature, and likely even diverge¹.

Our data is most naturally explained if there are disconnected local metallic regimes above T_C which form at the temperature T^* . This finding is consistent with earlier studies which have found significant ferromagnetic signals far above T_C ^{15,16}. The metallic regions may be either phase separated (and possibly static) domains, or they may be dynamic fluctuations of the metallic state. As temperature goes down and the whole system enters a metallic state, one may expect to see some physical parameters from fluctuations either diverge or show a

discontinuity. This however contradicts our observation. As will be shown later, one can see that there is no divergence or discontinuity as a function of temperature in our data. Therefore, we argue that our data is most consistent with the phase separation picture and one may be able to deconvolve the spectrum into the components which arise from the metal and non-metal portions. We can approximate this by subtracting the 180K EDC from all other EDCs as shown in figure 4b to create “metallic EDCs” or M-EDCs as shown in figure 4b. It should be pointed out that the slight variation of spectra from sample to sample, which has been commonly observed in ARPES, imperils the practice of extracting intrinsic properties from data of different samples. Therefore, we don't use the higher temperature data of figure 2c to do the subtraction as this is from a different sample. Figure 4c shows the same M-EDCs but scaled to all have the same amplitude. Within the noise, all the M-EDCs have similar lineshapes with coherent peaks near E_F and an incoherent background at high binding energy, though the widths of the M-EDC coherent peak (or low energy MDC peak) become broader with increasing temperature (figure 4d). The integrated spectral weight of the M-EDCs varies smoothly as a function of temperature, with no clear break at T_C (figure 4d). This, as well as the approximate temperature-independence of the M-EDC lineshape indicates that the electrons in the metallic regions have similar properties above and below T_C , and that temperature has surprisingly little effect on the behavior or interactions of electrons in the metallic regions. This is consistent with the approximate independence of v_F , λ , and m^* in the metallic regions shown in figure 4a. We do note, however, that the scattering rate increases significantly around and above T_C , as seen by the green triangles of figure 4c. This curve directly shows the scattering length or mean free path of the electrons, which is the inverse of the plotted MDC (momentum distribution curve) width. The temperature dependence of the MDC width may have contributions from a simple temperature broadening and the shrinking of metallic domains with temperature. How to deconvolve the two effects is still under investigation.

The picture that then arises is that metallic portions arise at a temperature T^* near room temperature, which also may be related to the temperature scale at which magnetic polarons freeze¹⁷. As the temperature is lowered the proportion of metallic portions grows until a critical ratio of metallic to insulating portions is reached. At that point electrons can percolate from one metallic region to another, bringing about the macroscopic metallic¹⁸ and ferromagnetic states, as well as being consistent with the “colossal” decrease in resistivity with an applied magnetic field. Above T_C individual domains are ferromagnetic, but the macroscopic random arrangements of these FM domains makes the whole system paramagnetic. The percolation effect at T_C can align these domains by the Hund's interaction between itinerant electrons and localized t_{2g} electrons and make

them behave collectively. Therefore the macroscopic FM emerges at the percolation temperature T_C . In the CMR effect, the “preformed” ferromagnetic metallic clusters just above T_C each have a large magnetic moment but are randomly oriented, and a relatively small magnetic field can then align the magnetic moment in these clusters, leading to a global ferromagnetic state, with percolation between these aligned clusters inducing metallicity. In certain models this behavior is expected from a competition between different phases, for example between the ferromagnetic metal phase and the charge-ordered antiferromagnetic insulating phase^{18,19,20}, though in contrast to ref 18, the materials used here are far away from the charge-ordered doping level. Therefore, even in these most homogeneous of manganites the tendency for electronic phase separation appears to be very strong. Theoretical arguments predict both the phase separation and the existence of a higher temperature scale T^{*21} , with ideas similar to the Griffiths singularity²² in which T^* would be the critical temperature of the associated clean system in the absence of disorder, and which have recently been discussed in the context of manganite physics^{21,23}. Further study is of course still needed to confirm whether this or other models are most appropriate to explain the experimental behavior. A T^* scale is one of the key properties of the high T_C superconductors, and has for years been the subject of intense controversy². In these compounds, disorder also appears to be highly relevant, especially in the underdoped regime where the T^* scale exists. In this case it signals the emergence of the pseudogap, which may be the precursor to the long range superconducting order which forms at T_C ²⁴ – a clear analogy to the manganites where T^* signals the emergence of the metallic domains which become long

range at T_C . Also similar to the cuprates, it appears that the T^* temperature scales may not be universal to all doping levels of the manganites. Pinning these details down and then understanding their implications will certainly be an area of intense study in the near future.

It is becoming increasingly clear that some of the most dramatic responses in modern materials occur in systems in which multiple phases or orders with similar energy scales compete with each other^{19,20,21,25}. It is then natural that in at least some of these systems spatial heterogeneities will occur, and small perturbations can cause drastic macroscopic alterations to the physical properties or even new types of “emergent” behavior. The key is finding which aspects of the inhomogeneity are intrinsic and what is their role in determining the key physical properties of the system.

In summary, using ARPES we show a new type of metal-insulator transition in solids in the colossal magnetoresistive oxide $La_{1.24}Sr_{1.76}Mn_2O_7$. In contrast to known cases, the unusual finding is that while $La_{1.24}Sr_{1.76}Mn_2O_7$ is globally insulating it is locally still a metal, with the local metal behavior forming at an even higher temperature – T^* . Our data indicates the important roles of phase separation and percolation effects.

The authors thank Y. Tokura and T. Kimura for providing preliminary samples and are grateful to D. N. Argyriou, A. Bansil, E. Dagotto, A. Moreo, R. Osborn, D. Reznik, Y. Tokura for helpful discussions. This work was supported by the U.S. Department of Energy under grant DE-FG02-03ER46066 and by the U.S. National Science Foundation grant DMR 0402814. The ALS is operated by the Department of Energy, Office of Basic Energy Sciences.

* zsun@lbl.gov

† Dessau@colorado.edu

- ¹ M. Imada, A. Fujimori, and Y. Tokura, Rev. Mod. Phys. **70**, 1039 (1998).
- ² T. Timusk and B. Statt, Rep. Prog. Phys. **62**, 61 (1999).
- ³ Q. A. Li, K. E. Gray, and J. F. Mitchell, J.F. Phys. Rev. B **59**, 9357 (1999).
- ⁴ Z. Sun et al., Phys. Rev. Lett. **97**, 056401 (2006).
- ⁵ D. S. Dessau et al., Phys. Rev. Lett. **81**, 192 (1998).
- ⁶ Y.-D. Chuang et al., Science **292**, 1509 (2001).
- ⁷ T. Saitoh et al., Phys. Rev. B **62**, 1039 (2000).
- ⁸ N. Mannella et al., Nature **438**, 474 (2005).
- ⁹ D. S. Dessau et al., Phys. Rev. Lett. **66**, 2160 (1991).
- ¹⁰ Z. -X. Shen and D. S. Dessau, Phys. Rep. **253**, 1 (1995).
- ¹¹ A. Damascelli, Z. Hussain, and Z. -X. Shen, Rev. Mod. Phys. **75**, 473 (2003).
- ¹² J. Voit, Rep. Prog. Phys. **57**, 977 (1995).

¹³ J.W. Allen, Sol. State Comm. **123**, 469 (2002).

¹⁴ C.M. Varma, Phys. Rev. B **54**, 7328 (1996).

¹⁵ D. N. Argyriou, et al., J. Appl. Phys. **83**, 6374 (1998).

¹⁶ R. Osborn, et al., Phys. Rev. Lett. **81**, 3964 (1998).

¹⁷ D.N. Argyriou, et al., Phys. Rev. Lett. **89**, 36401 (2002).

¹⁸ M. Uehara, et al., Nature **399**, 560 (1999).

¹⁹ E. Dagotto, Science **309**, 257 (2005).

²⁰ Y. Tokura, Rep. Prog. Phys. **69**, 797 (2006).

²¹ J. Burgu, et al., Phys. Rev. Lett. **87**, 277202 (2001).

²² R.B. Griffiths, Phys. Rev. Lett. **23**, 17 (1969).

²³ M. B. Salamon, P. Lin, and S. H. Chun, Phys. Rev. Lett. **88**, 197203 (2002).

²⁴ V.J. Emery, and S.A. Kivelson, Nature **374**, 434 (1995).

²⁵ S. Murakami, and N. Nagaosa, Phys. Rev. Lett. **90**, 197201 (2003).